Molecular Crystals
Publication details, including instructions for authors and subscription information:
http://www.tandfonline.com/loi/gmcl15

Band Structure and Current Carriers Mobilities in Imidazole Crystal

H. Chojnacki [a] & A. Gołębiewski [b]

[a] Department of Physical Chemistry, Wroclaw Technical University Wrochaw, Wyb., Wyspia[ngrave]skiego, 27, Poland

[b] Department of Theoretical Chemistry, Jagiellonian University Kraków, Krupnicza, 41, Poland

Version of record first published: 21 Mar 2007.

To cite this article: H. Chojnacki & A. Gołębiewski (1969): Band Structure and Current Carriers Mobilities in Imidazole Crystal, Molecular Crystals, 5:4, 317-330

To link to this article: http://dx.doi.org/10.1080/15421406908082941

Molecular Crystals and Liquid Crystals. 1969. Vol. 5, pp. 317–330

Printed in Great Britain

Band Structure and Current Carriers Mobilities in Imidazole Crystal

H. CHOJNACKI

Department of Physical Chemistry, Wrocław Technical University
Wrocław, Wyb. Wyspiańskiego 27
Poland

A. GOŁĘBIEWSKI

Department of Theoretical Chemistry, Jagiellonian University
Kraków, Krupnicza 41
Poland

Abstract—Molecular orbital method in the tight binding approximation has been applied to imidazole crystal. Using STO's the excess hole and electron band structures were determined for the two positions of proton of the hydrogen bond corresponding to extreme resonance structures. The μ_{bb},$\mu_{a'a'}$, anisotropy of current carriers mobilities in the constant relaxation time is in fair agreement with experimental data. There is, however, no agreement for the $\mu_{cc}/\mu_{a'a'}$ ratio. Possible origins of this discrepancy are discussed.

One line of theoretical attack on the mobility problem in organic semiconductors is the tight binding approximation of the band theory. Such an approach, with theoretically evaluated resonance integrals, was used in order to explain the anisotropy of current carriers mobilities in some benzenoid hydrocarbon crystals.[6,9,16] A semi-empirical model of the tight binding approximation was also applied for biological systems.[8,18,19] In the last papers, however, the anisotropy of current carriers mobilities has not been discussed.

In this paper we discuss the purely theoretical approach of the tight binding model in application to imidazole crystal. The unit cell of this crystal comprises four molecules (Fig. 1) and belongs to the C_{2h}^5—$P2_1/c$ space group.[10] The molecules, linked by hydrogen bonds of 2.86 Å in length, form infinite chains extending along the c axis. The twisting angle between π-

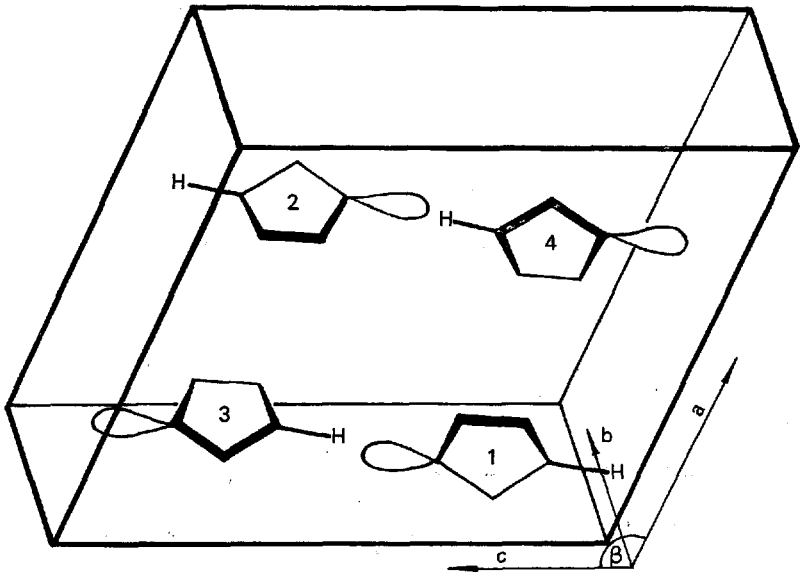

Figure 1. Schematic representation of the unit cell of imidazole crystal according to the Martinez-Carrera data[10] with the numbering of molecules.

orbitals of two adjacent molecules in the chain is equal to 61.5°. The conductivity is approximately the same along the **b** and **c** axes but smaller by a factor of 3.6 along the **a** axis.[14] In the (010) plane the hydrogen bridges alignment is close to the **c** axis and the maximal current corresponds to the hydrogen bonds direction. For the (100) plane, however, where the hydrogen bonds make an angle of $\pm 25.5°$ with the **c** axis, no current anisotropy is observed.

It is believed that the proton of the hydrogen bond may assume two stable positions within the bond and a tunneling effect can occur between the two potential minima with frequency of order 10^9 cps.[1] The collective motion of protons of hydrogen bridges may be important for charge migration in the crystal lattice. The molecular structure of imidazole in the crystalline state can also be described as a resonance hybrid of the two extreme forms

(Fig. 2).[2] It seems to be a justification for the calculation performed for the two extreme resonance structures with the same atom coordinates except those of the hydrogen bond proton and with the respective π-electronic charge distribution.

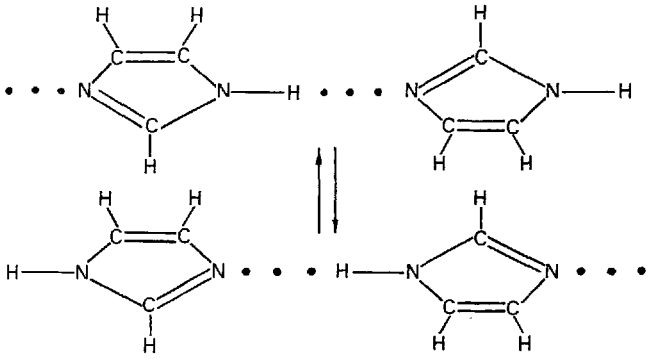

Figure 2. Resonance forms of imidazole.

(a) The Approximation Used

Within the frame work of the tight binding approximation the crystal orbitals were constructed as a linear combination of molecular π-orbitals of imidazole

$$\psi(\mathbf{r}) = \sum_{\mathbf{n}} \sum_{s} c_{\mathbf{n},s} \psi_s(\mathbf{r} - \mathbf{r}_{\mathbf{n}} - \mathbf{r}_s) \tag{1}$$

where $\psi_s(\mathbf{r} - \mathbf{r}_{\mathbf{n}} - \mathbf{r}_s)$ is the highest occupied or the lowest empty π-orbital of imidazole molecule described by indices $\mathbf{n} = (n_a, n_b, n_c)$ and s. Molecular orbitals different in s have in general different orientations in the crystal lattice. Vector $\mathbf{r}_{\mathbf{n}}$ shows the center of a unit cell described by indices n_a, n_b, n_c. Vector $\mathbf{r}_s$ is directed from the center of the cell to the geometric center of the s-th molecule within the cell ($s = 1, 2, 3, 4$).

SCF LCAO MO orbitals calculated in the Pariser–Parr–Pople approximation[13] were used for molecular orbitals in our calculation (Table 1). Assuming the zero differential overlap

TABLE 1 Highest Occupied and Lowest Unoccupied Molecular Orbitals of Imidazole Molecule

Molecular Orbital	Orbital Energy (eV)	c_{r1}	c_{r2}	c_{r3}	c_{r4}	c_{r5}
Highest Occupied	− 8.2767	0.0001	0.5072	0.3686	− 0.4529	− 0.6339
Lowest Unoccupied	1.2818	0.3472	− 0.6820	0.4352	0.1953	− 0.4322

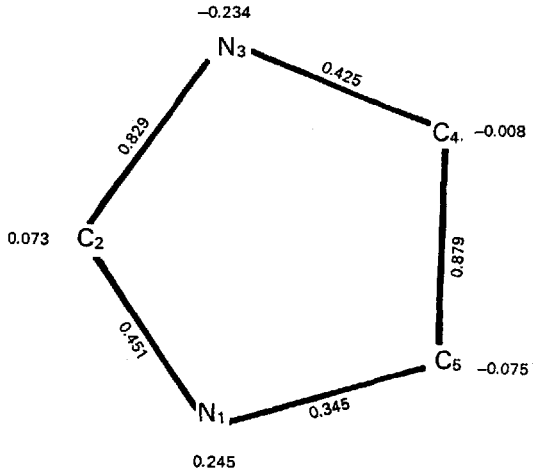

Figure 3. π-electronic charge densities and bond orders for imidazole molecule.

Coulomb repulsion integrals were calculated from the Mataga–Nishimoto approximation[12] with $(ii \mid ii) = I_i - A_i$. The ionization potentials I_i and the electron affinities were taken from the Hinze and Jaffé data.[5] The resonance integrals β_{ij} were found from the Kon's formula,[7] taking β_{ij} equal to -2.39 eV for C—C bond and

$R = 1.379$ Å, $\beta_{ij} = -2.576$ eV for C—N bond and $R = 1.34$ Å, $\beta_{ij} = -2.35$ eV for N—N bond and $R = 1.33$ Å. The geometrical structure of the imidazole molecule was assumed in accordance with the X-ray studies of Martinez-Carrera for room temperature.[10]

We assume that the Hamiltonian H, appropriate for an excess electron or hole, has the form (in a.u.)

$$H = -1/2\nabla^2 + U(\mathbf{r}) = -1/2\nabla^2 + \sum_{\mathbf{n}} \sum_{s} V_s(\mathbf{r} - \mathbf{r}_{\mathbf{n}} - \mathbf{r}_s) \tag{2}$$

The eigenevalue problem is then reduced to a set of linear equations

$$\sum_{\mathbf{n}} \sum_{s} c_{\mathbf{n},s} H_{st}(\mathbf{n},\mathbf{m}) = E \sum_{\mathbf{n}} \sum_{s} c_{\mathbf{n},s} S_{st}(\mathbf{n},\mathbf{m}) \tag{3}$$

where

$$H_{st}(\mathbf{n},\mathbf{m}) = \int \psi_t^*(\mathbf{r} - \mathbf{r}_{\mathbf{m}} - \mathbf{r}_t) H \psi_s(\mathbf{r} - \mathbf{r}_{\mathbf{n}} - \mathbf{r}_s)\, dV \tag{4}$$

$$S_{st}(\mathbf{n},\mathbf{m}) = \int \psi_t^*(\mathbf{r} - \mathbf{r}_{\mathbf{m}} - \mathbf{r}_t) \psi_s(\mathbf{r} - \mathbf{r}_{\mathbf{n}} - \mathbf{r}_s)\, dV \tag{5}$$

According to the Bloch theorem we have

$$\sum_{s} \{ \sum_{\mathbf{n}} [H_{st}(\mathbf{n},\mathbf{m}) - E S_{st}(\mathbf{n},\mathbf{m})] \exp(i\mathbf{k}\cdot\mathbf{r}_{\mathbf{n}}) \} c_s = 0 \tag{6}$$

for any value of t and $\mathbf{m}$. In what follows we take $t = 1$ and $\mathbf{m} = \mathbf{0} = (0,0,0)$. Neglecting overlap integrals and taking into account symmetry elements of the imidazole unit cell (center of inversion and a glide plane) we get

$$\begin{pmatrix} E_{us} \\ E_{gs} \\ E_{ua} \\ E_{ga} \end{pmatrix} = \sum_{\mathbf{n}} \exp(i\mathbf{k}\cdot\mathbf{r}_{\mathbf{n}}) \cdot \begin{pmatrix} 1 & 1 & 1 & 1 \\ 1 & 1 & -1 & -1 \\ 1 & -1 & 1 & -1 \\ 1 & -1 & -1 & 1 \end{pmatrix} \cdot \begin{pmatrix} H_{11}(\mathbf{n},\mathbf{0}) \\ H_{21}(\mathbf{n},\mathbf{0}) \\ H_{31}(\mathbf{n},\mathbf{0}) \\ H_{41}(\mathbf{n},\mathbf{0}) \end{pmatrix} \tag{7}$$

If we neglect resonance integrals for atoms being more than 5 Å apart then we may write

$$\begin{pmatrix} E_{us} \\ E_{gs} \\ E_{ua} \\ E_{ga} \end{pmatrix} = 2 \cdot \begin{pmatrix} 1 & 1 & 1 & 1 \\ 1 & 1 & -1 & -1 \\ 1 & -1 & 1 & -1 \\ 1 & -1 & -1 & 1 \end{pmatrix} \times \begin{pmatrix} H_{11}(\mathbf{0},\mathbf{0}) \\ H_{21}(\mathbf{0},\mathbf{0}) \cdot \cos[\mathbf{k} \cdot (\mathbf{a} - 2\mathbf{x} + \mathbf{b} - 2\mathbf{y} + \mathbf{c} - 2\mathbf{z})] \\ H_{31}(\mathbf{0},\mathbf{0}) \cdot \cos[\mathbf{k} \cdot (0.5\mathbf{b} - 2\mathbf{y} + 0.5\mathbf{c})] \\ H_{41}(\mathbf{0},\mathbf{0}) \cdot \cos[\mathbf{k} \cdot (\mathbf{a} - 2\mathbf{x} + 0.5\mathbf{b} + 0.5\mathbf{c} - 2\mathbf{z})] \end{pmatrix} + 2 \cdot \begin{pmatrix} 1 & 0 & 0 & 0 \\ 0 & 1 & 0 & 0 \\ 0 & 0 & 1 & 0 \\ 0 & 0 & 0 & 1 \end{pmatrix} \cdot H_{11}(\mathbf{u},\mathbf{0}) \cdot \cos[\mathbf{k} \cdot \mathbf{b}] \tag{8}$$

where as the origin of the coordinate system the geometric center of molecule 1 was taken and vector **u** has the components **u** = (0,1,0). Vectors **x**,**y**,**z** are standard coordinates for molecule 1 of the imidazole space group.

The resonance integrals $H_{11}(\mathbf{0},\mathbf{0})$, $H_{21}(\mathbf{0},\mathbf{0}), \ldots, H_{11}(\mathbf{u},\mathbf{0})$ were calculated theoretically expressing π-electron molecular orbitals in terms of Slater type atomic orbitals with the exponents 3.08 and 3.69 for carbon and nitrogen respectively.[3] The Hamiltonian potential energy terms were reduced according to the Goeppert-Mayer and Sklar approximation.[4] Neglecting the small excess charges on individual atoms of the imidazole molecule and using the Slater type orbitals we have what follows

$$V(\mathrm{H}) = -\frac{e^{-2r}}{r}(1 + r) \tag{9}$$

for hydrogen atoms of hydrogen bonds

$$V(\mathrm{C}) = -\frac{e^{-2\beta}}{r}(4 + 6\beta + 4\beta^2 + 4/3\beta^3) \tag{10}$$

for carbon atoms, where $\beta = \alpha r$. Besides

$$V(\mathrm{N_{pyrrole}}) = -\frac{e^{-2\beta}}{r}(5 + 15/2\beta + 5\beta^2 + 5/3\beta^3) + 3/2(3\cos^2\theta - 1)R(r,\beta) \quad (11)$$

for nitrogen atoms of pyrrolic type, where θ is an angle between the axis of the $2p\pi$ orbital and vector **r** directed from the nitrogen atom towards the reference point, and

$$V(\mathrm{N_{pyridine}}) = -\frac{e^{-2\beta}}{r}(5 + 15/2\beta + 5\beta^2 + 5/3\beta^3) + Q(r,\beta)\cos\theta + R(r,\beta)\cdot(3\cos^2\theta - 1) \quad (12)$$

for nitrogen atoms of pyridine type, where θ is an angle between the axis of the sp^2-type lone pair and vector **r**. Furthermore

$$Q(r,\beta) = \frac{5\sqrt{6}}{9\beta r}[1 - e^{-2\beta}(1 + 2\beta + 2\beta^2 + 6/5\beta^3 + 2/5\beta^4)] \quad (13)$$

$$R(r,\beta) = \frac{1}{\beta^2 r}[1 - e^{-2\beta}(1 + 2\beta + 2\beta^2 + 4/3\beta^3 + 2/3\beta^4 + 2/9\beta^5)] \quad (14)$$

The resonance integrals which involve $V(\mathrm{N_{pyrrole}})$ and $V(\mathrm{N_{pyridine}})$ potentials were evaluated with the help of two-dimensional Gaussian integration using 16^2 points. Three-center integrals which involve those of the hydrogen bond $V(\mathrm{H})$-type potentials, were evaluated with the use of the Mulliken approximation.[11]

(b) Discussion

The values of intermolecular resonance integrals for holes and electrons for the two resonance structures of imidazole are given in Table 2. The appropriate band structures in a reduced Bril-

louin zone are shown in Figs. 4–9. As expected the bands are split into four Davydov components except the a axis direction where only two branches are obtained. In some cases, however,

TABLE 2 Intermolecular Resonance Integrals Calculated for the Two Resonance Structures of the Imidazole Crystal (in units of 10^{-4}eV)

	Imidazole-1 (Standard Position of the HB Proton)		Imidazole-2 (Reversed Position of the HB Proton)	
Integral Type	Hole	Electron	Hole	Electron
$H_{21}(0,0)$	0.03	0.01	0.01	0.00
$H_{31}(0,0)$	0.15	12.97	− 2.68	5.97
$H_{41}(0,0)$	20.07	− 25.52	23.25	10.17
$H_{11}(u,0)$‡	− 28.99	5.02	− 30.38	10.34

‡ Vector **u** has the components (0,1,0).

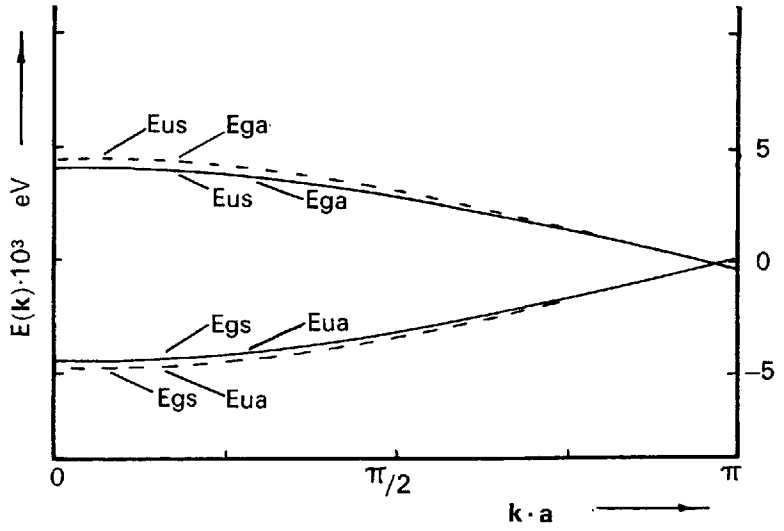

Figure 4. Shape of the excess hole band in the a^{-1} direction for standard (solid line) and reversed position of proton in the hydrogen bond (dashed line).

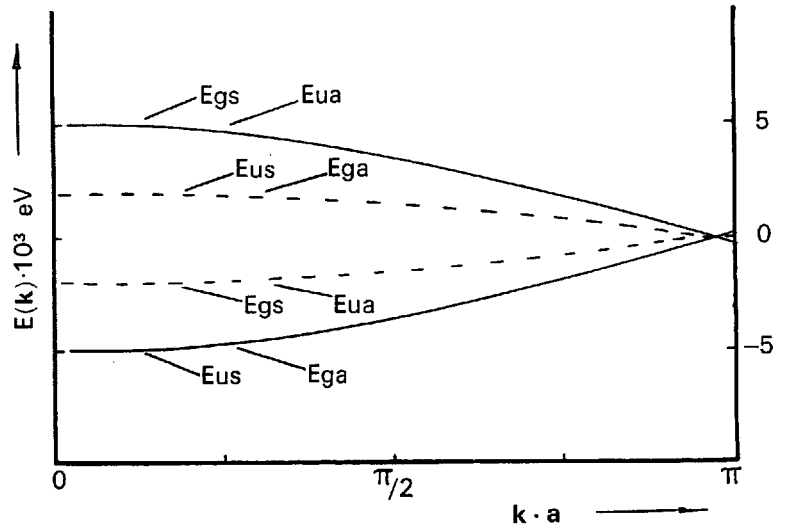

Figure 5. Shape of the excess electron band in the $\mathbf{a}^{-1}$ direction for standard (solid line) and reversed position of proton in the hydrogen bond (dashed line).

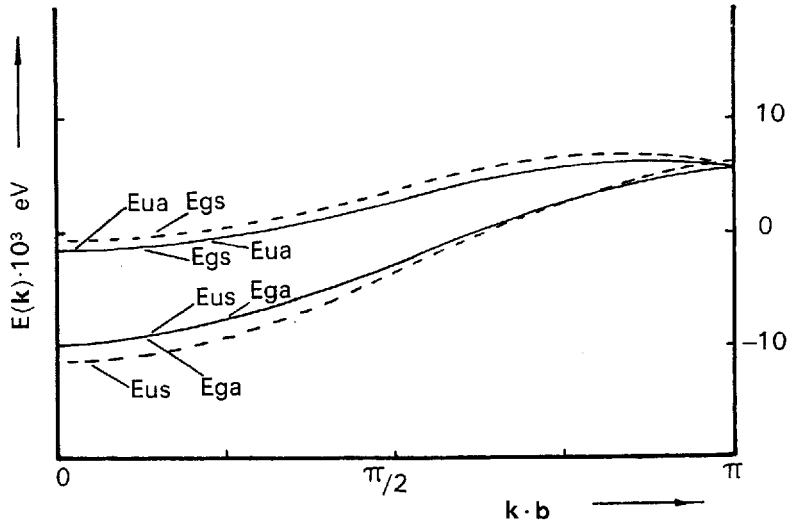

Figure 6. Shape of the excess hole band in the $\mathbf{b}^{-1}$ direction for standard (solid line) and reversed positions of proton in the hydrogen bond (dashed line).

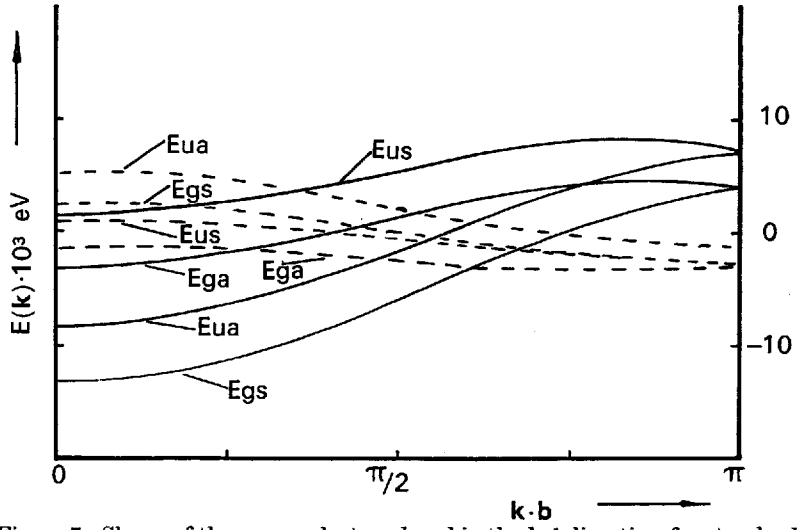

Figure 7. Shape of the excess electron band in the $\mathbf{b}^{-1}$ direction for standard (solid line) and reversed position (dashed line) of proton in the hydrogen bond.

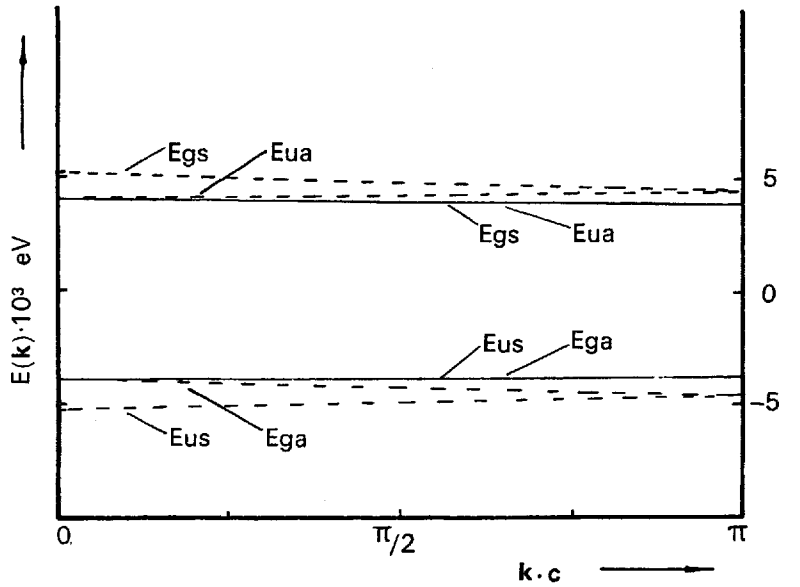

Figure 8. Shape of the excess hole band in the $\mathbf{c}^{-1}$ direction for standard (solid line) and reversed position (dashed line) of proton in the hydrogen bond.

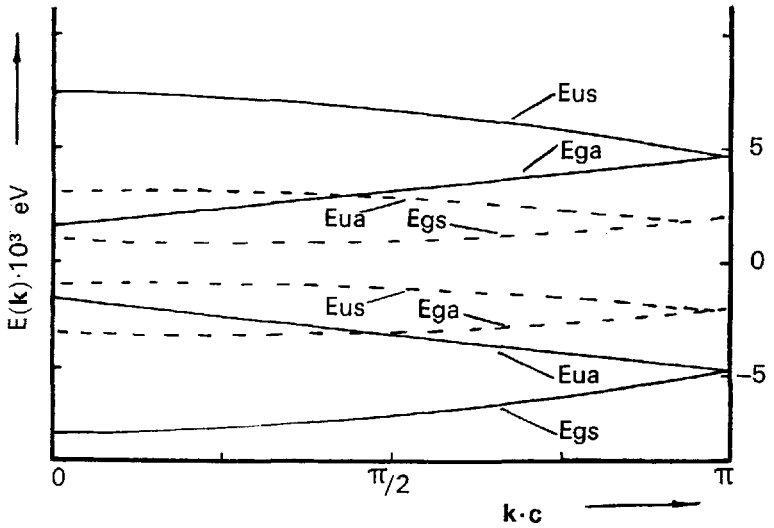

Figure 9. Shape of the excess electron band in the c^{-1} direction for standard (solid line) and reversed position (dashed line) of proton in the hydrogen bond.

the splittings of E_{us}— E_{ga} and E_{gs}— E_{ua} are too small to be indicated in the above figures. The estimated bandwidths of the components are smaller than 0.01 eV being of similar order as those of anthracene.[9] They are much smaller than calculated by Ladik and Appel[8] for polynucleotides (0.24–0.76 eV) as well as those of Yomosa et al.[19] for hydrogen bonded polypeptides. Higher values of resonance integrals evaluated by the last authors empirically may be responsible for their wider bandwidths. It will be noted that the role of the three-center integrals is not significant and is similar order to the effect of hydrogens on the band structures of naphthalene crystals.[17]

The calculated band structure allows one to estimate the components of the mobility tensor providing an assumption regarding the relaxation time is made. Assuming a constant free time, we find the values of μ_{ij} from the relation

$$\mu_{ij} = e\tau\langle v_i v_j\rangle/kT \tag{15}$$

where $v_i = 1/\hbar \operatorname{grad}_i E_i(\mathbf{k})$ is dependent on the component of the band. $\langle v_i v_j \rangle$ is the average value over four components of the imidazole band for all possible values of $\mathbf{k}$ calculated according to the LeBlanc scheme.[9]

The relative anisotropies of the mobility tensor are given in Table 3. Here we compare with experiment the values of $\mu_{bb}/\mu_{a^1a^1}$ and $\mu_{cc}/\mu_{a^1a^1}$ found for holes and electrons for the two extreme positions of proton in the hydrogen bond. It can be seen that a fair agreement with experimental data is observed in the case of the a^1b plane where $\pi - \pi$ interactions seem to be decisive. For the (010) plane, however, the calculated anisotropy is lower than that from experiment. Thus it seems that the method does not consider the role of hydrogen bonding satisfactorily.

We see several possible ways of analyzing this effect. One might, for example, try to include $2p$ orbitals of hydrogen atoms in the expansion used for crystal orbitals (1). Another possibility lies in the coupling of the charge carrier transfer with the oscillatory tunneling of protons in the network of hydrogen bonds. Such an oscillation is hardly expected for the ground state but there are strong arguments in favour of the tunneling process in the excited states as well as for cations and anions.[15] These two possible explanations are the subject of a further analysis.

The numerical part of this work has been performed on the Elliott 803 B digital computer.

The authors wish to express their indebtedness to Prof. Dr. K. Pigoń for revision of the manuscript.

TABLE 3 Calculated Anisotropy of the Current Carriers Mobilities in the Imidazole Crystal and a Comparison with the Experimental Relative Conductivity at Room Temperature

	Imidazole-1		Imidazole-2		Arithmetic Mean for the Two Extreme Positions of Proton in HB		Relative Experimental Conductivity
Ratio	Hole	Electron	Hole	Electron	Hole	Electron	
$\mu_{bb}/\mu_{a^1a^1}$‡	6.27	0.84	5.25	3.53	5.76	2.19	3.6
$\mu_{cc}/\mu_{a^1a^1}$‡	0.06	0.62	0.09	0.80	0.08	0.71	3.6

‡ The $\mathbf{a}'$ is the axis perpendicular to the (100) plane.

REFERENCES

1. Brickman, J., *Ber. Buns. Ges.* (Zeitschr. f. Elektrochem.) **70**, 157, 521 (1966).
2. Brown, G. P. and Aftergut, S., *J. Chem. Phys.* **38**, 1356 (1963).
3. Eyring, H., Walter, J. and Kimball, G. E., *Quantum Chemistry*, New York London 1958.
4. Goeppert-Mayer, M. and Sklar, A. L., *J. Chem. Phys.* **6**, 645 (1938).
5. Hinze, J. and Jaffé, H. H., *J. Am. Chem. Soc.* **84**, 540 (1962).
6. Katz, J. L., Rice, S. A., Choi, S. and Jortner, J., *J. Chem. Phys.* **39**, 1683 (1963).
7. Kon H., *Bull. Chem. Soc. Japan* **28**, 275 (1955).
8. Ladik, J. and Appel, K., *J. Chem. Phys.* **40**, 2470 (1964).
9. LeBlanc, O. H., Jr., *J. Chem. Phys.* **35**, 1275 (1961).
10. Martinez-Carrera, S., *Acta Cryst.* **20**, 783 (1966).
11. Mulliken, R. S., *J. Chim. Phys.* **46**, 497 (1944).
12. Mataga, N. and Nishimoto, K., *Z. Physik. Chem.*, Neue Folge **13**, 140 (1957).
13. Parr, R. G., *The Quantum Theory of Molecular Electronic Structure*, W. A. Benjamin, Inc., New York Amsterdam 1964.
14. Pigoń, K. and Chojnacki, H., *Acta Phys. Polon.* **31**, 1069 (1967).
15. Rein, R. and Harris, F. E., *J. Chem. Phys.* **42**, 2177 (1965).
16. Silbey, R., Jortner, J., Rice, S. A. and Vala, M. T., Jr., *J. Chem. Phys.* **43**, 2925 (1965).
17. Tanaka, K. and Niira, K., *J. Phys. Soc. Japan* **24**, 520 (1968).
18. Yomosa, S., *J. Phys. Soc. Japan* **19**, 1718 (1964); ibid. **18**, 1494 (1963).
19. Yomosa, S., Miyata, T. and Suzuki, H., *J. Phys. Soc. Japan* **24**, 878 (1968).